

AD 660892

Basal Plane Emittance of Pyrolytic Graphite at Elevated Temperatures

JULY 1967

Prepared by **ROBERT J. CHAMPETIER**
Materials Sciences Laboratory
Laboratory Operations
AEROSPACE CORPORATION

Prepared for **SPACE AND MISSILE SYSTEMS ORGANIZATION**
AIR FORCE SYSTEMS COMMAND
LOS ANGELES AIR FORCE STATION
Los Angeles, California



THIS DOCUMENT HAS BEEN APPROVED FOR PUBLIC
RELEASE AND SALE; ITS DISTRIBUTION IS UNLIMITED

Reproduced by the
CLEARINGHOUSE
for Federal Scientific & Technical
Information Springfield, Vt. 02151

46

**Air Force Report No.
SAMSO-TR-67-5**

**Aerospace Report No.
TR-0158(3250-20)-10**

**BASAL PLANE EMITTANCE OF PYROLYTIC GRAPHITE
AT ELEVATED TEMPERATURES**

**Prepared by
Robert J. Champelier
Materials Sciences Laboratory**

**Laboratory Operations
AEROSPACE CORPORATION**

July 1967

**Prepared for
SPACE AND MISSILE SYSTEMS ORGANIZATION
AIR FORCE SYSTEMS COMMAND
LOS ANGELES AIR FORCE STATION
Los Angeles, California**

**This document has been approved for public
release and sale; its distribution is unlimited.**

FOREWORD

This report is published by the Aerospace Corporation, El Segundo, California, under Air Force Contract No. F04695-67-C-0158 and documents research carried out from 19 January 1964 to 19 December 1966. It was submitted on 12 September 1967 to Captain William D. Bryden, Jr., SMTRE for review and approval.

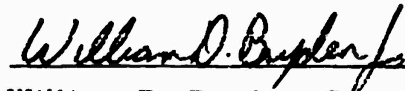
The author wishes to thank Mr. J. D. McClelland, who suggested the study and closely followed its progress, Dr. J. Kaspar, who contributed in the analysis of the method and in numerous enlightening discussions, Mr. R. F. Schneidmiller, who performed the electron microscopy and diffraction, and Mr. D. L. Whitney, who helped develop the equipment. Grateful acknowledgements also go to Mr. W. E. Moore, whose assistance was invaluable in all phases of the experimental preparations and in taking data.

Approved



W. C. Riley, Director
Materials Sciences Laboratory
Laboratory Operations

Publication of this report does not constitute Air Force approval of the report's findings or conclusions. It is published only for the exchange and stimulation of ideas.



William D. Bryden, Jr., Capt., USAF
Project Officer

ABSTRACT

A direct measurement of the total hemispherical emittance of "as deposited" PG layers on ATJ graphite cylinders in the range from 1200 to 2840°C is described. The method consisted of resistively heating these long, thin cylinders inside a cooled, blackened enclosure until the power generated was all radiated and temperature equilibrium ensued. By sighting an optical pyrometer through a window in the enclosure, the apparent temperature of the surface and the true temperature of a cavity inside the samples could be measured. These temperatures, as well as the electrical power supplied to the sample, were recorded for each equilibrium temperature. These data for various sample thicknesses were used to determine the true temperature of the surface, the total hemispherical emittance ϵ_H , and the normal emittance at 0.65 μ . The electrical resistivity in the ab-plane and the thermal conductivity in the c-direction were also determined. The ϵ_H for PG was approximately 0.6 μ from 1300 to 2600°C. Exposure for a few seconds in an inert atmosphere or in a vacuum to temperatures above 2600°C, irreversibly altered the surface finish and increased ϵ_H to progressively higher values, depending on the time and temperature. The normal emittance values at 0.65 μ also were significantly affected.

CONTENTS

FOREWORD	ii
ABSTRACT	iii
I. INTRODUCTION	1
II. GENERAL APPROACH	3
A. Emittances	3
B. Resistivity in the ab-Plane	4
C. Thermal Conductivity in the c-Direction	4
D. Data Reduction	6
III. EXPERIMENT	11
A. Apparatus	11
B. Samples	11
C. Experimental Errors	13
IV. RESULTS	17
A. Surface Finish Alteration	17
B. Normal Spectral Reflectance at Room Temperature	24
C. Normal Emittance at 0.65μ	26
D. Total Hemispherical Emittance	30
E. Thermal Conductivity in the c-Direction	30
F. Electrical Resistivity in the ab-Plane	33
V. CONCLUDING REMARKS	37
REFERENCES	39

FIGURES

1. $\Delta T_{PG1}, \Delta T_{PG2}, \Delta T_{PG}$, and ΔT_{ATJ} vs t	8
2. Calculated ΔT_{PG} vs f(t)	10
3. Sketch of Apparatus	12

FIGURES (Continued)

4.	PG Sample, Potential Probes, and the Three Pyrometer Sight Holes	14
5.	Cross-Sectional View of a Typical PG-ATJ Sample	15
6.	PG Sample After High-Temperature Exposure in Argon	18
7.	PG Sample with Extreme Surface Changes After High-Temperature Exposure in Argon (A Potential Probe and the Bottom Yoke Failed)	19
8.	Electron Micrographs of PG Surfaces Before and After High-Temperature Exposure in Argon (Replicating Technique)	20
9.	Electron Micrograph of Peeled-Off Surface Material from Sample Subject to High-Temperature Exposure in Argon	21
10.	Electron Diffraction Patterns of: (a) Post-Exposure Surface Material, (c) Highly Oriented Graphite, and (b) and (d) Gold Standards	23
11.	Spectral Reflectance at 18-deg Incidence of PG Surfaces After Various Exposures	25
12.	Typical Plot at ΔT_{obs} vs T_i	27
13.	Typical Plot of Measured W vs T_i	28
14.	Examples of $(\Delta T_{\text{obs}} - \Delta T_{\text{ATJ}})$ vs $f(t)$ Plots.	29
15.	Total Hemispherical Emittance and Normal Emittance of PG Samples at 0.65μ	31
16.	Systematic Errors in ϵ_H for a Typical Sample	32
17.	Thermal Conductivity of PG Cylindrical Sample in Radial (c-Axis) Direction	34

FIGURES (Continued)

18.	Electrical Resistivity in ab-Direction Calculated from Four PG Shell and PG-ATJ Samples with $t \approx 0.3$ mm	35
19.	Electrical Resistivity in the ab-Direction Calculated for a PG-ATJ Sample with Medium Thickness ($t \approx 0.081$ mm)	36

I. INTRODUCTION

Pyrolytic graphite, a highly oriented form of graphite, has properties that make it a desirable material for reentry nose cone applications. These properties include mechanical strength, low thermal conductivity in a direction normal to the deposition surface, and oxidation resistance. Prediction of the thermal history of nose cones during reentry requires knowledge of trajectory and material parameters, in particular, the thermal radiation characteristics. With the Stefan-Boltzmann law, the total hemispherical emittance ϵ_H can be directly used to calculate the total power that the skin radiates in all directions and at all wavelengths for a given surface temperature.

Total hemispherical emittance data for pyrolytic graphite (PG) are not available at the present time. Measurements have been made in a direction normal to the deposition surface (i. e., in the c-direction); however, all but two of these measurements were made at temperatures below 1850°C. Pears'¹ work ranged up to 2150°C, and Marple's,² to 2240°C. Since Pears' measurements were made in a heated furnace, emittance changes in the first few seconds could not be recorded. In addition, the assumption that PG is grey (i. e., that the spectral emittance at the 0.65- μ optical pyrometer wavelength has the same value as ϵ_H) was not verified. Marple used a monochromator that received energy along the c-direction of the heated sample and compared it to that from a cavity in the sample. He obtained values of the spectral normal emittance $\epsilon_N(\lambda)$ over the wavelength range of 0.45 to 2.8 μ , which includes about 80% of the radiated energy at 2240°C. Calculation of ϵ_H from Marple's data requires knowledge of the directional emittance as a function of angle of emission at several wavelengths. These data are not available. An alternative approach would be to calculate the directional emittance of a single crystal of graphite from its optical constants

and to use this information to calculate a conservative lower ϵ_H limit for the PG. Again, the optical constants have been measured only over a fraction of the wavelength and temperature ranges needed.

The experimental effort described in this report is based on a novel approach and has resulted in a direct measurement of ϵ_H from 1200 to $\sim 2800^\circ\text{C}$. Other properties of PG samples were also measured over the same temperature range, including normal emittance at the standard 0.65μ wavelength used in optical pyrometers, thermal conductivity in the c-direction, and electrical resistivity in the ab-plane.

II. GENERAL APPROACH

A. EMITTANCES

The samples were made by depositing PG layers of several thicknesses onto the outside surface of ATJ graphite hollow cylinders (1-cm diameter and 20-cm long). Each sample was centered in a water-cooled, blackened chamber and each end of the sample was held by water-cooled electrodes. When a constant electrical current was passed through a sample, the ohmic heating caused the temperature to increase until the power generated was completely radiated. The current running through the sample and the voltage drop through the center section, where the temperature profile was flat, were then recorded. Simultaneously, optical pyrometer sightings were made through a window in the chamber wall. The apparent, or brightness, temperature T_o' of the outside surface of the sample, i. e., the PG surface, was recorded; the true temperature inside the sample T_1 was measured through a small hole drilled in the sample wall. By a comparison of these data obtained at surface temperatures from 1200 to 2800°C on samples with different PG thicknesses, the ΔT_ϵ between the brightness and true temperatures of the PG surface T_o' and T_o , was obtained for each equilibrium temperature.

With T_o' and ΔT_ϵ known, their sum immediately gave T_o , and the normal emittance of 0.65 μ was obtained from the well-known equation

$$\ln \epsilon_N (0.65 \mu) = (c_2/\lambda) \left[(1/T_o) - (1/T_o') \right] \quad (1)$$

The ϵ_H values were then calculated using the Stefan-Boltzmann law for blackbody radiation

$$W_{BB} = A\sigma T_o^4 \quad (2)$$

and the definition

$$\epsilon_H = (W_{PG}/W_{BB}) T_o \quad (3)$$

where W_{PG} is the power radiated by the section of the sample between the voltage probes, which were a measured distance apart and defined a radiating area A.

B. RESISTIVITY IN THE ab-PLANE

The samples were removed from the emissometer at the completion of each run, sliced, and their dimensions measured under an optical comparator. The thickness of each PG film was measured under a microscope with a graduated scale in one eyepiece that was calibrated with a ruled standard.

The geometry of the ATJ mandrels was measured before deposition of PG and after the samples were sliced. The mandrel resistance was calculated using resistivity data* from similar ATJ cylinders. Thus, for each sample and at each temperature, the difference of the total measured current and the calculated ATJ current I_{ATJ} gave the current I_{PG} through the PG, permitting an evaluation of the resistivity along the length of the PG cylindrical layer, i. e., in the ab-plane.

C. THERMAL CONDUCTIVITY IN THE c-DIRECTION

The measurements also yielded thermal conductivity k_c in the radial direction, which is also the c-axis for the PG cylindrical layers.

* R. J. Champetier and W. E. Moore, Emittance Calorimeter and Its Use in Determining Thermal Emittance and Conductivity of ATJ Graphite (to be published).

Since the true temperatures of the outer PG surface and of the inside of the ATJ were known for each sample and at any radiated power, the additional information needed for calculating k_c was the temperature at the PG/ATJ interface and the power generated within the ATJ. If perfect contact at the interface of the two graphites were maintained, then the temperature difference observed with the pyrometer ΔT_{obs} would be

$$\Delta T_{obs} \equiv T_i - T_o'$$

$$\Delta T_{obs} = \Delta T_{ATJ} + \Delta T_{PG} + \Delta T_{\epsilon} \quad (4)$$

where the last term represents the correction for ϵ_N (0.65μ) of the PG surface that was determined previously. The first term is calculated from the known current distribution, the thermal conductivity k_{ATJ} , determined in a previous study,^{*} and the geometry of the ATJ mandrel, corrected for thermal expansion. Using the steady-state heat flow equation for uniform power generation within the walls of a cylinder

$$\Delta T_{ATJ} = \frac{EI_{ATJ}}{2\pi l k_{ATJ}} \left(\frac{1}{2} - \frac{D_i^2}{D_o^2 - D_i^2} \ln \frac{D_o}{D_i} \right)_{ATJ} \quad (5)$$

where l represents the distance between the voltage probes across which the electrical potential E is measured, and D_i and D_o represent the inside and outside diameters of the ATJ. The values of k_{ATJ} that had been determined previously were for the same ATJ orientation as used here, i.e., "with the grain."

In obtaining Eq. (5) by integration over all radii, the current density was assumed constant within the ATJ. This assumption is not strictly

* R. J. Champetier and W. E. Moore, *Emittance Calorimeter and Its Use in Determining Thermal Emittance and Conductivity of ATJ Graphite* (to be published).

correct since the resistivity is a function of temperature, and a radial temperature gradient exists. It was found that a correct calculation differs from the results of Eq. (5) by less than 1%, which is quite acceptable here since ΔT_{ATJ} is typically much smaller than ΔT_{PG} and the uncertainties in k_{ATJ} are $\pm 20\%$.

Similarly, the term ΔT_{PG} in the case of a film of PG with an infinitesimal thickness would be

$$\Delta T_{PG} = \frac{E}{2\pi t k_c} \left[I_{PG} \left(\frac{1}{2} - \frac{D_i^2}{D_o^2 - D_i^2} \ln \frac{D_o}{D_i} \right) + I_{ATJ} \ln \frac{D_o}{D_i} \right] \quad (6)$$

Here, the first term in the brackets is similar to that for ATJ in Eq. (5), and the second represents the additional temperature gradient necessary for the heat generated within the ATJ to flow steadily through the cooler PG. D_i in Eq. (6) now refers to the inside diameter of the PG and D_o to its outside diameter. A differential dT_{PG} based on Eq. (6) could be written and an integration performed over t provided the resistivity in the ab-direction and k_c remain constant over the temperature range. Since these restrictions are not fulfilled, Eq. (6) was tested for the case of thick films by a more exact numerical integration. The approximation in ΔT_{PG} using Eq. (6) was within 0.6% of the correct value for the worst case and, therefore, deemed adequate.

Once ΔT_ϵ is determined, Eqs. (4) and (6) can be solved for k_c and values obtained directly.

D. DATA REDUCTION

In principle, Eq. (4) can be used to get all the information required at any one temperature by using only two samples with different t values. The assumption needs to be made that k_c , ρ_{ab} , $\epsilon_N(0.65 \mu)$, and ϵ_H are alike for the two samples. Data obtained at equal T_o , and therefore ΔT_ϵ , are used and Eq. (4) immediately gives

$$(\Delta T_{PG})_1 - (\Delta T_{PG})_2 = \text{constant}$$

which again can be solved directly for k_c . In the present application, however, a number of samples were used with a range of t values in order to determine the repeatability and uncover possible systematic errors.

The ΔT_{obs} data were compared at equal W_{PG} levels, and also at equal T_i levels. It was possible to evaluate changes in ϵ_H and ϵ_N (0.65μ) that took place as a result of high-temperature exposure.

The various terms in Eqs. (4) and (6) are plotted as a function of t in Fig. 1 and are from a calculation based on typical sample parameters, with the assumption that all the samples have the same T_o , ϵ_H , and ϵ_N (0.65μ). The first term in Eq. (6) has been labeled ΔT_{PG1} and the second term ΔT_{PG2} .

At a common value of EI, the data for the various samples differing in t can be compared by plotting $\Delta T_{obs} - \Delta T_{ATJ}$, which is equivalent to $\Delta T_{PG} + \Delta T_{\epsilon}$ by Eq. (4), vs a function $f(t)$ of the thickness. This function, derived theoretically* is linear with ΔT_{PG} (i. e., $f(t) = k \Delta T_{PG}$ where k is a constant proportional to k_c). The derivation is subject to the restrictions, appropriate in this application, that $t/D_i \ll 1$ and that the ratio ρ_{PG}/ρ_{ATJ} of the resistivities changes slowly with temperature. Thus a plot of $(\Delta T_{PG} + \Delta T_{\epsilon})$ vs $f(t)$ has for its $f(t) = 0$ intercept, the value of ΔT_{ϵ} (i. e., ΔT_{PG} vanishes at $t = 0$, leaving the emittance correction ΔT_{ϵ}).

The validity of the derived $f(t)$ for the t/D_i corresponding to the thickest samples was tested by plotting the ΔT_{PG} calculated from typical

* R. J. Champetier, Total Hemispherical Emittance and Normal Emittance at 0.65μ of Pyrolytic Graphite Cylinders from 1500 to 3000 K by a Calorimetric Method, Aerospace Corp. (to be published).

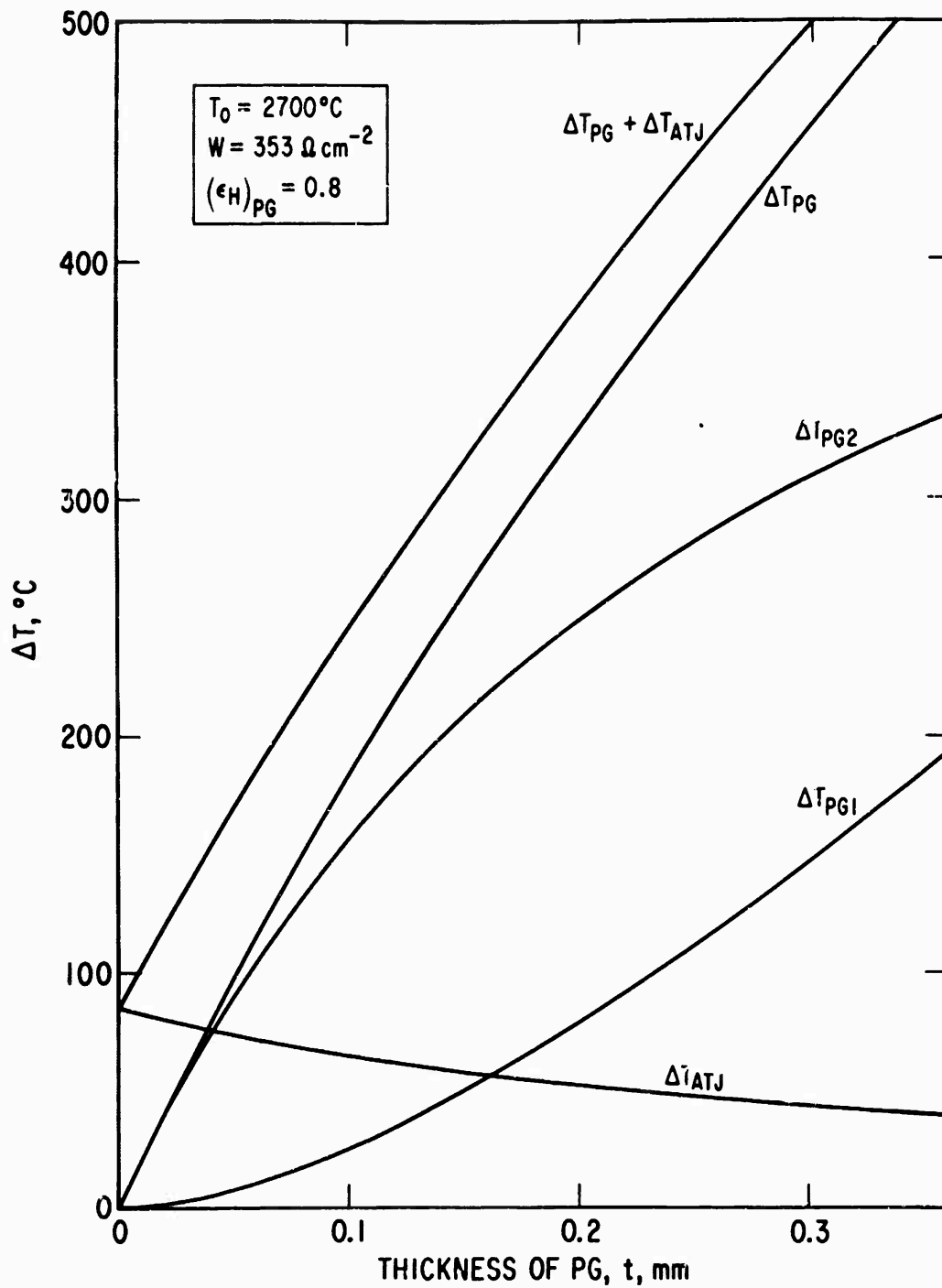


Fig. 1. ΔT_{PG1} , ΔT_{PG2} , ΔT_{PG} , and ΔT_{ATJ} vs t .

k_c , ρ_{PG} , and ϵ_H data against $f(t)$. The departure from a straight-line fit was less than 3°C (Fig. 2).

In data reduction, the observed temperatures were corrected for the transmission of the window in the chamber; then for each sample, l_{ATJ} , ΔT_{ATJ} , and l_{PG} were computed. The results of $(\Delta T_{obs} - \Delta T_{ATJ})$ were plotted against $f(t)$ for fixed W values. Upper and lower lines bounding the scatter of the data points were used to estimate uncertainties in ΔT_ϵ .

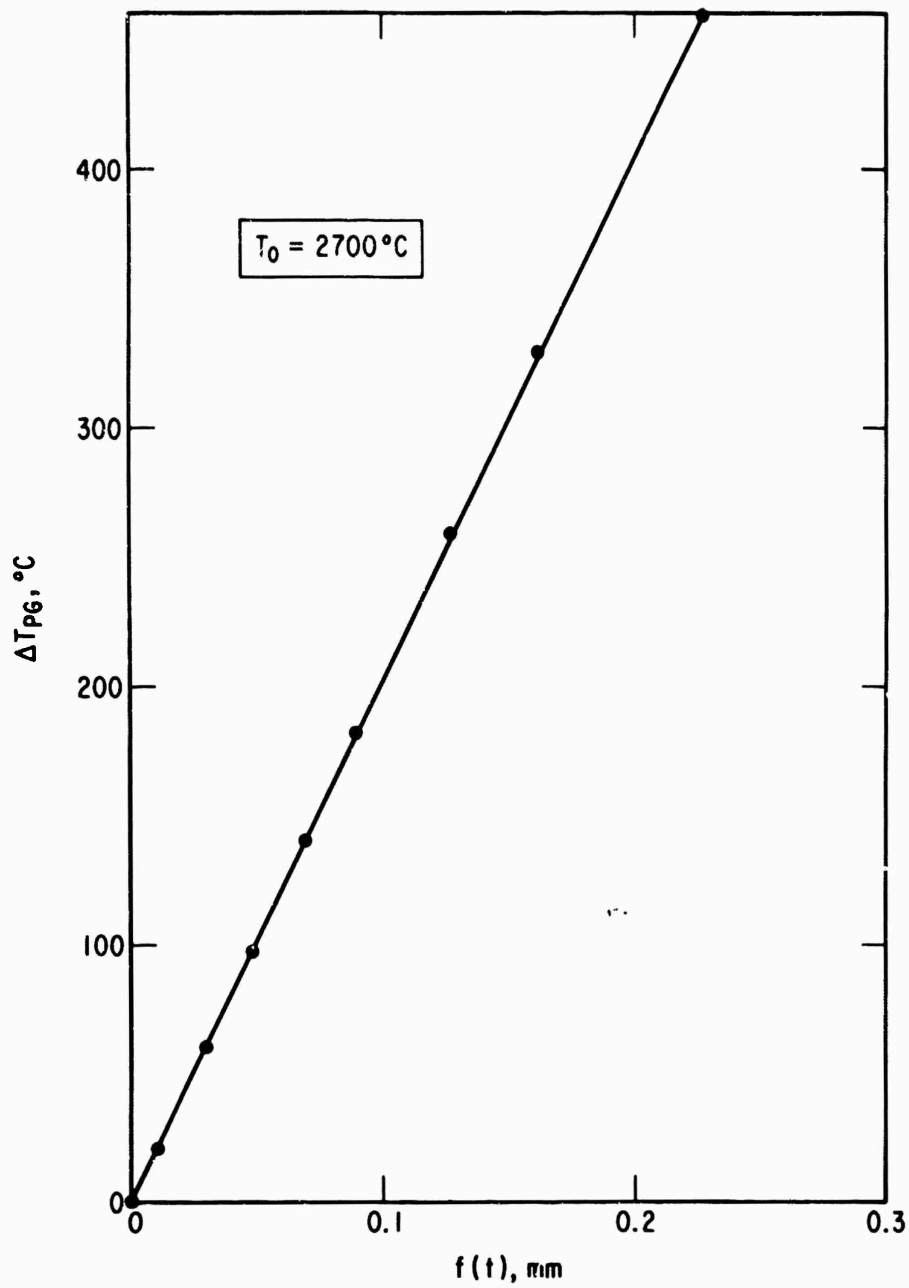


Fig. 2. Calculated ΔT_{PG} vs $f(t)$.

III. EXPERIMENT

A. APPARATUS

The chamber (Fig. 3) was carefully designed* so that none of the sample radiation would reflect off the walls and be reabsorbed by the PG. Whenever the PG was heated, the chamber was either in a vacuum or contained argon. Oxidants were removed by passing the argon through a 4-ft column of titanium chips at 900°C. The vacuum was obtained after several argon flushings with a well-trapped diffusion pump. The silicone pump oil used has a vapor pressure below 10^{-8} Torr at room temperature. The entire system pressure could be set at any point between 10^{-6} Torr and 1 atm absolute. Thus, it is felt that the sample was heated in an unreactive environment. The pressures used were always controlled so as to cause negligible convection errors as determined experimentally.*

The optical pyrometer, a micro-optical unit,** was checked frequently against similar units, calibrated by NBS.

The 60-cps supplied power was regulated to 0.1% to a T_0 of $\sim 2400^\circ\text{C}$ and was unregulated above that. All voltmeters were frequently checked by standard methods that use thermal transfer standards, five-dial potentiometers, and saturated standard cells.

B. SAMPLES

The ATJ substrates were sanded to a smooth finish before PG deposition. The deposition of PG was performed by the Super-Temp

* R. J. Champetier and W. E. Moore, Emittance Calorimeter and Its Use in Determining Thermal Emittance and Conductivity of ATJ Graphite (to be published).

** The Pyrometer Instrument Company, Inc., Bergenfield, New Jersey.

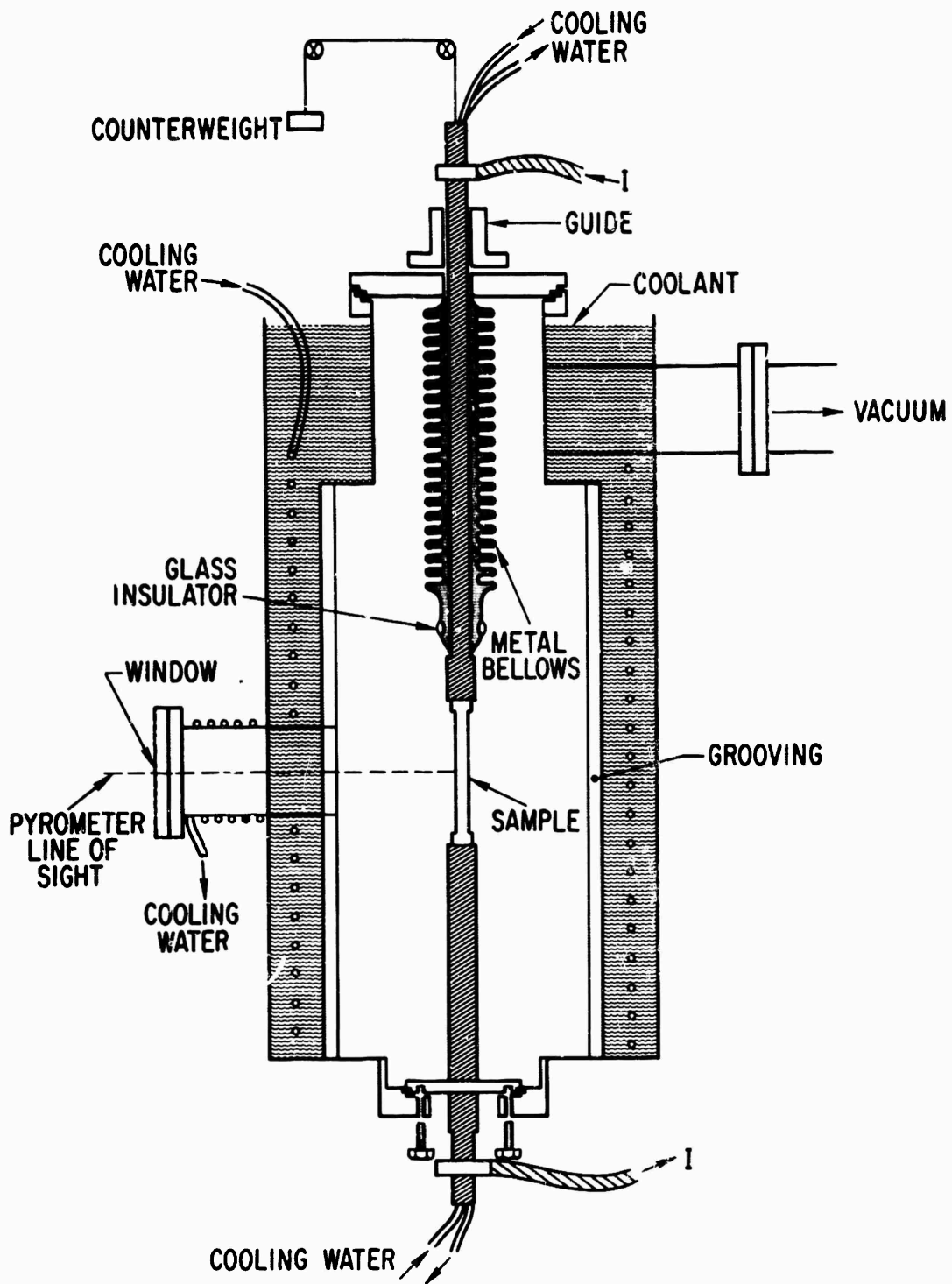


Fig. 3. Sketch of Apparatus.

Corporation.* Standard manufacturing procedures were used in forming the PG; special attention was given to obtaining a good PG/ATJ bond on the very first deposition layers. After PG deposition, the entire furnace was allowed to cool before it was opened and the samples exposed to the atmosphere. The surfaces were not touched, and the samples were placed in the emissometer chamber with no further surface treatment. The installation of the voltage probes, which were carbon filaments, was made under a microscope and without touching the sample. A sample readied for the emissometer is shown in Fig. 4 and typical cross sections in Fig. 5.

C. EXPERIMENTAL ERRORS

An effort was made to investigate major sources of uncertainty in the final answers. The assumption was made that the current density within the PG layer is essentially uniform, although the current electrodes were in contact with the ATJ substrate only. A convincing room-temperature test was performed for an extreme case. A plate of PG, 2-in. square by 0.2-in. thick, with its c-axis along the 0.2-in. side, was fastened to two electrodes set 2-in. apart on one of the large faces. An electrical current of 15 A was passed through the plate. The voltage difference between two points, ~ 0.5 in. apart, was then measured at several locations. It was found that within 1% (the precision of the voltmeter), the voltage difference and, therefore, the current density was the same on both sides of the plate halfway between the electrodes. A similar test was performed, also at room temperature, on a sample with the thickest PG layer; similar results were obtained.

The time-temperature exposures were slightly below the levels that cause significant dimensional changes, such as those observed by Richardson and Zehms.³

* Santa Fe Springs, California

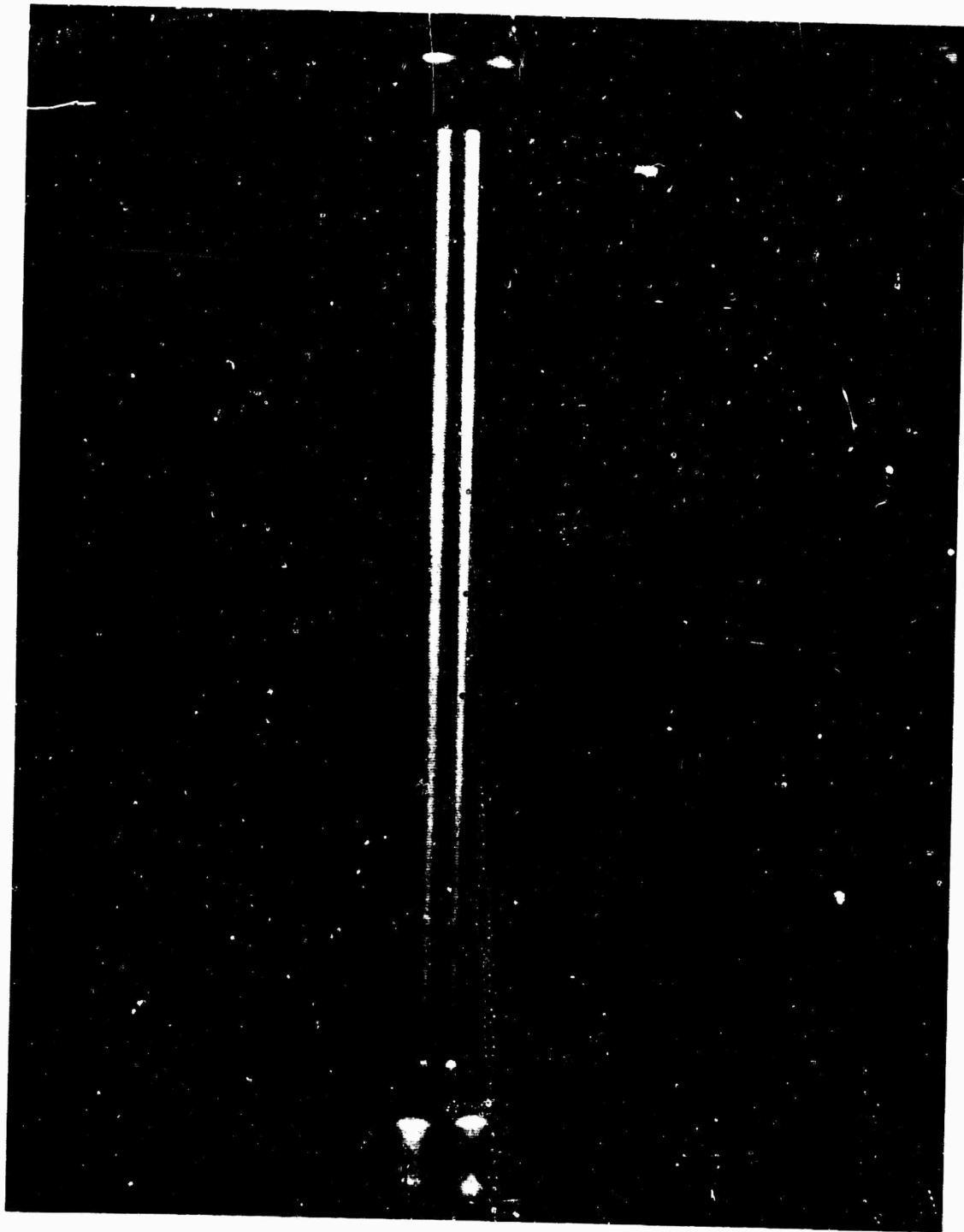


Fig. 4. PG Sample, Potential Probes, and the Three Pyrometer Sight Holes.

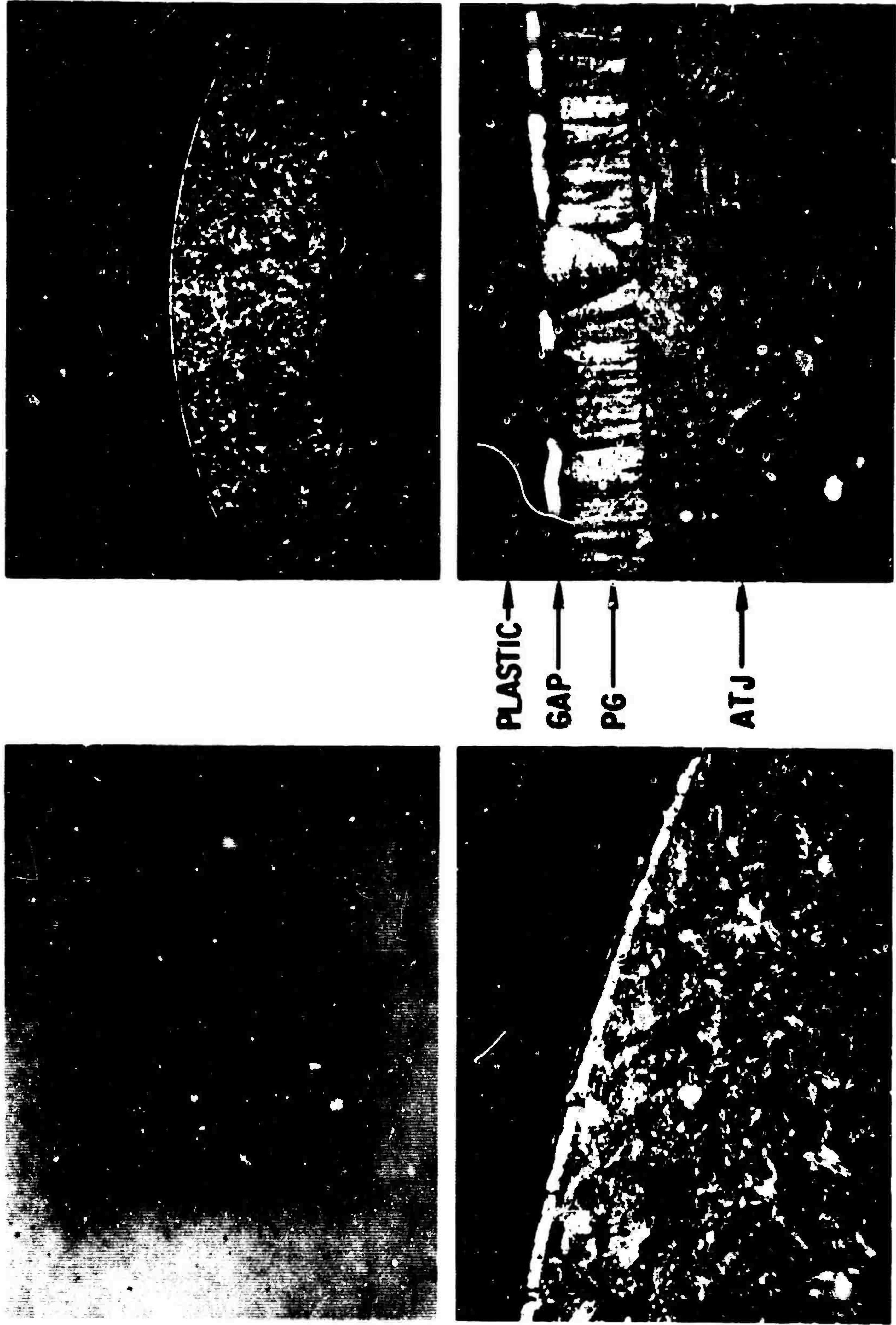


Fig. 5. Cross-Sectional View of a Typical PG-ATJ Sample.

Slight errors in the geometry of the ATJ substrate were significant in the evaluation of ρ_{ab} for the thickest PG layers (~ 0.3 mm) and resulted in very large scatter in the ρ_{ab} of the thinnest layers (~ 0.03 mm).

ATJ thermal conductivity data* are sufficiently accurate for this study considering the geometrical uncertainties. The $\pm 20\%$ spread in previous k_{ATJ} values resulted in ϵ_N (0.65μ) uncertainties of < 0.01 below 2000°C and increased to 0.02 at 2400°C and 0.03 at 2800°C . These, in turn, caused an uncertainty of about 0.005 in ϵ_H throughout the temperature range.

The ΔT_{obs} values for any one sample were typically reproducible within $\pm 10\%$; this limitation was largely due to the matching precision of the observer and the time allowed for the measurement.

* R. J. Champetier and W. E. Moore, Emittance Calorimeter and Its Use in Determining Thermal Emittance and Conductivity of ATJ Graphite (to be published).

IV. RESULTS

A. SURFACE FINISH ALTERATION

When exposed to temperatures in excess of 2450°C even for a few seconds in an inert atmosphere or in a vacuum, the surface of PG loses its shiny metallic appearance and becomes more deeply etched as the time and temperature level of the exposure are increased. The nature of these changes was investigated by optical and electron microscopy. Samples that exhibit extreme surface change as a result of exposure to surface temperatures near 2800°C are shown in Figs. 6 and 7. Comparison with the shiny material near the cooled ends and with the unexposed sample in Fig. 4 reveals the extent of the change. The alteration in appearance was due to a roughening of the surface; the grain of which was slightly below the level of resolution of optical microscopy. Figure 8 shows the surface change as seen with an electron microscope using replicating techniques. Figure 9 shows electron microphotographs of the surface material itself that was removed after a high-temperature run. The PG sublimed in a nonuniform manner. These surface irregularities are of the order of $1\ \mu$. Surface changes above that magnitude were not observed.

The PG was deposited so as to obtain very small growth cones; i. e., the thicknesses were kept at 0.3 mm or less. The resulting surfaces, while not always typical of those on very thick PG layers, were uniform in temperature. No local variations or hot spots were discernible with the optical pyrometer, with a 0.05-mm resolution at the working distance.

Since the topographical variations of etched surface are $\sim 1\ \mu$, changes in the spectral reflectance and emittance should be significant from visible wavelengths into the near infrared. Indeed the appearance

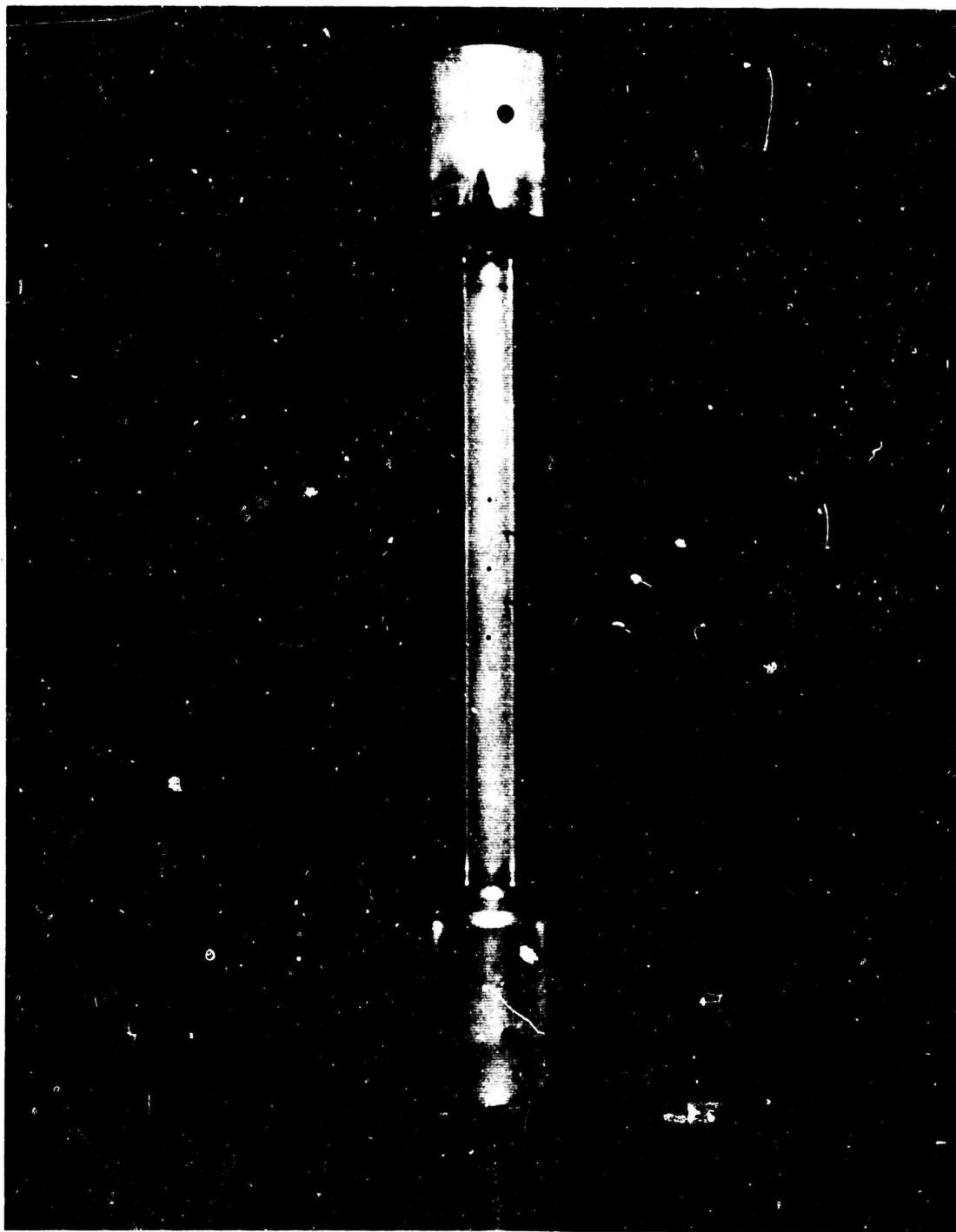


Fig. 6. PG Sample After High-Temperature Exposure in Argon.

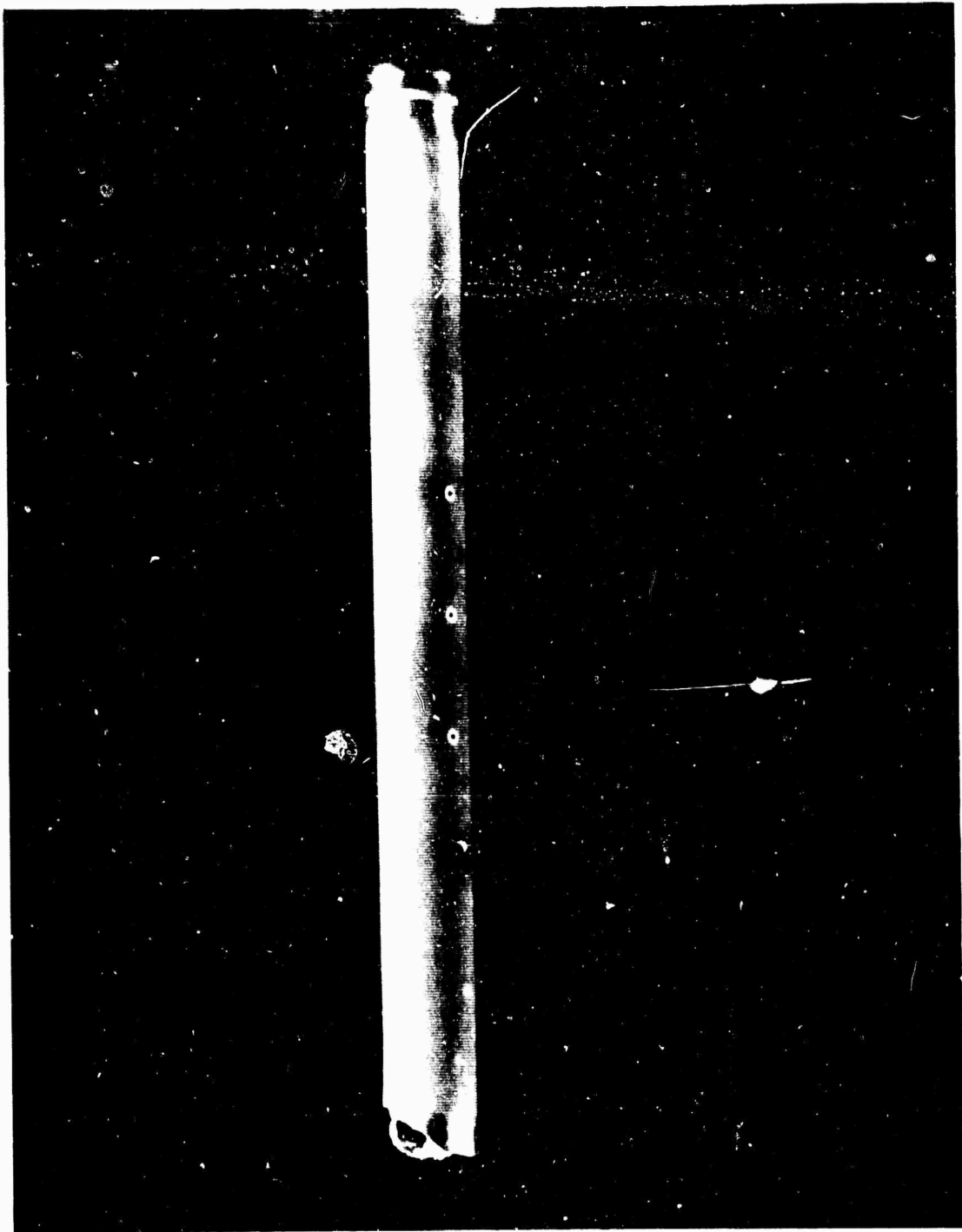


Fig. 7. FG Sample with Extreme Surface Changes After High-Temperature Exposure in Argon (A Potential Probe and the Bottom Yoke Failed).

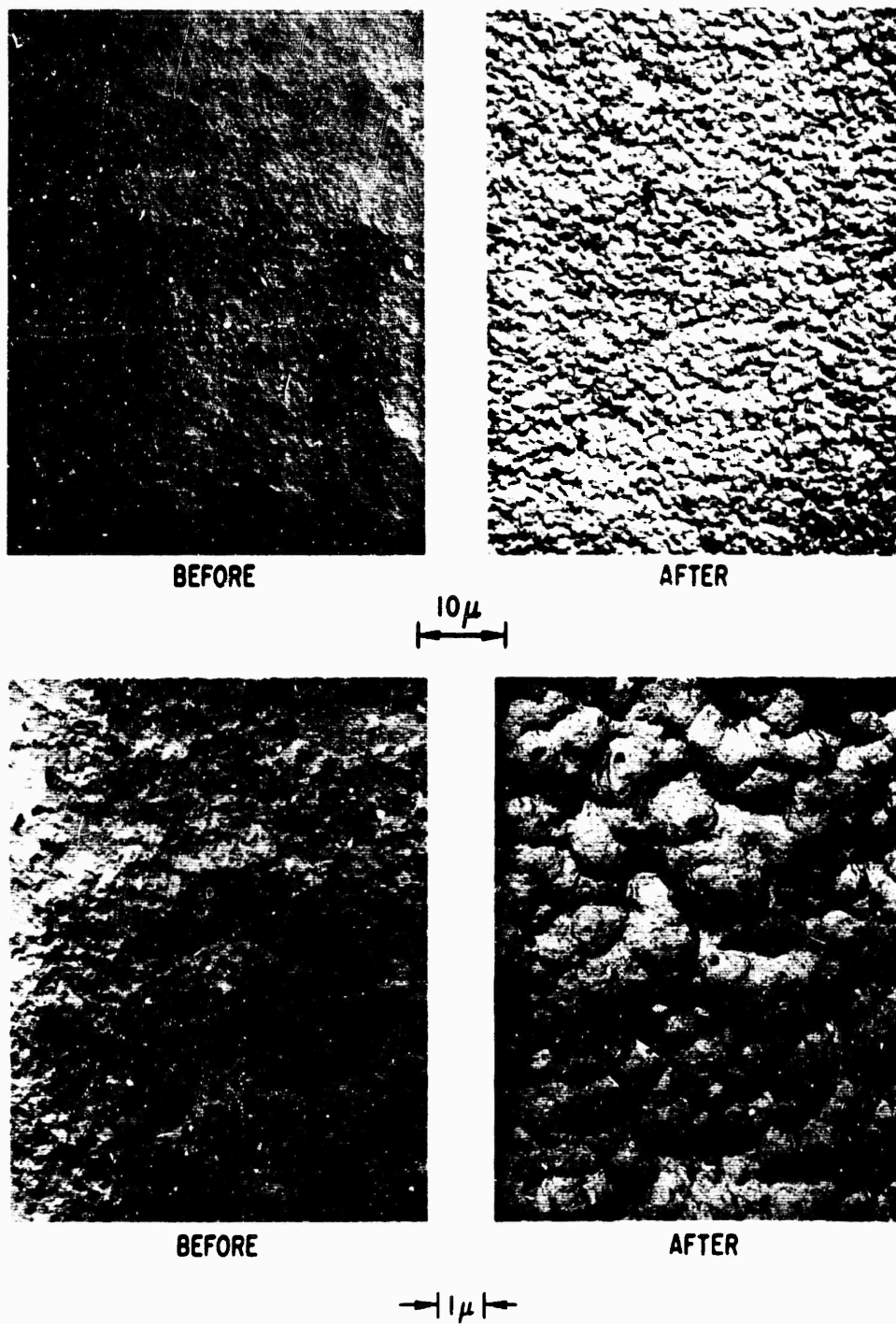


Fig. 8. Electron Micrographs of PG Surfaces Before and After High-Temperature Exposure in Argon (Replicating Technique).

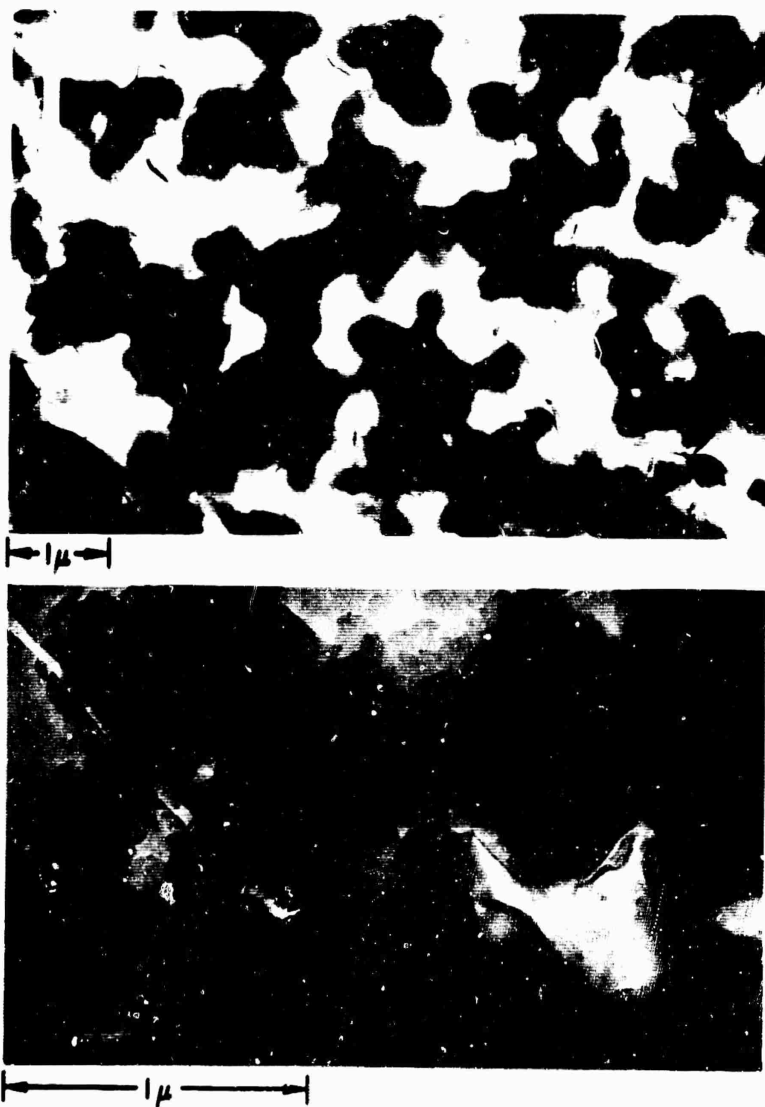


Fig. 9. Electron Micrograph of Peeled-Off Surface Material from Sample Subject to High-Temperature Exposure in Argon.

to the eye, i. e., in the 0.4 to 0.8- μ range, is quite different. Furthermore, the total hemispherical emittance should be significantly increased at elevated temperatures.

In some cases, extreme roughening was observed in which the entire surface had receded several microns except for about 10% of the area exclusively concentrated on the major growth cones, which themselves had receded but to a comparatively small degree. These cases were discarded as not typical and are ascribed to the resistive heating method used, whereby any physical isolation of a growth cone would be accentuated; i. e., since the current density through it would be lower, its temperature would also be lower, and it would not sublime as fast as the surrounding surface. Careful checking was done to verify the validity of the observed surface etching and to eliminate the possibility of an effect due to the apparatus. The techniques included (1) argon deoxidation, (2) use of a trapped 10^{-6} Torr vacuum, (3) spectrographic analyses of the affected PG surfaces, (4) spectrographic analyses of the carbon sublimed and subsequently condensed on cold surfaces, (5) electron diffraction (Fig. 10) of PG surface material seen in Fig. 9, and (6) systematic heating of the sample to determine where the changes occurred in the temperature cycles.

The etching occurred in both the vacuum and in argon; the surface luster could be restored, however, in oxygen. One possible explanation is that the sublimation and oxidation rates differ in their temperature dependencies. For sublimation the rate of surface removal near 2700°C varies as T^n where $n \sim 32$ for a heat of sublimation of ~ 180 kcal/mole. For oxidation $0 < n < 5$ based on oxidation rates to 1900°C . The crystalline and growth-cone patterns could result in minute temperature nonuniformities at the surface because of the very high radial temperature gradients. Hence on a microscopic scale, adjacent surface points would sublime at somewhat different rates,

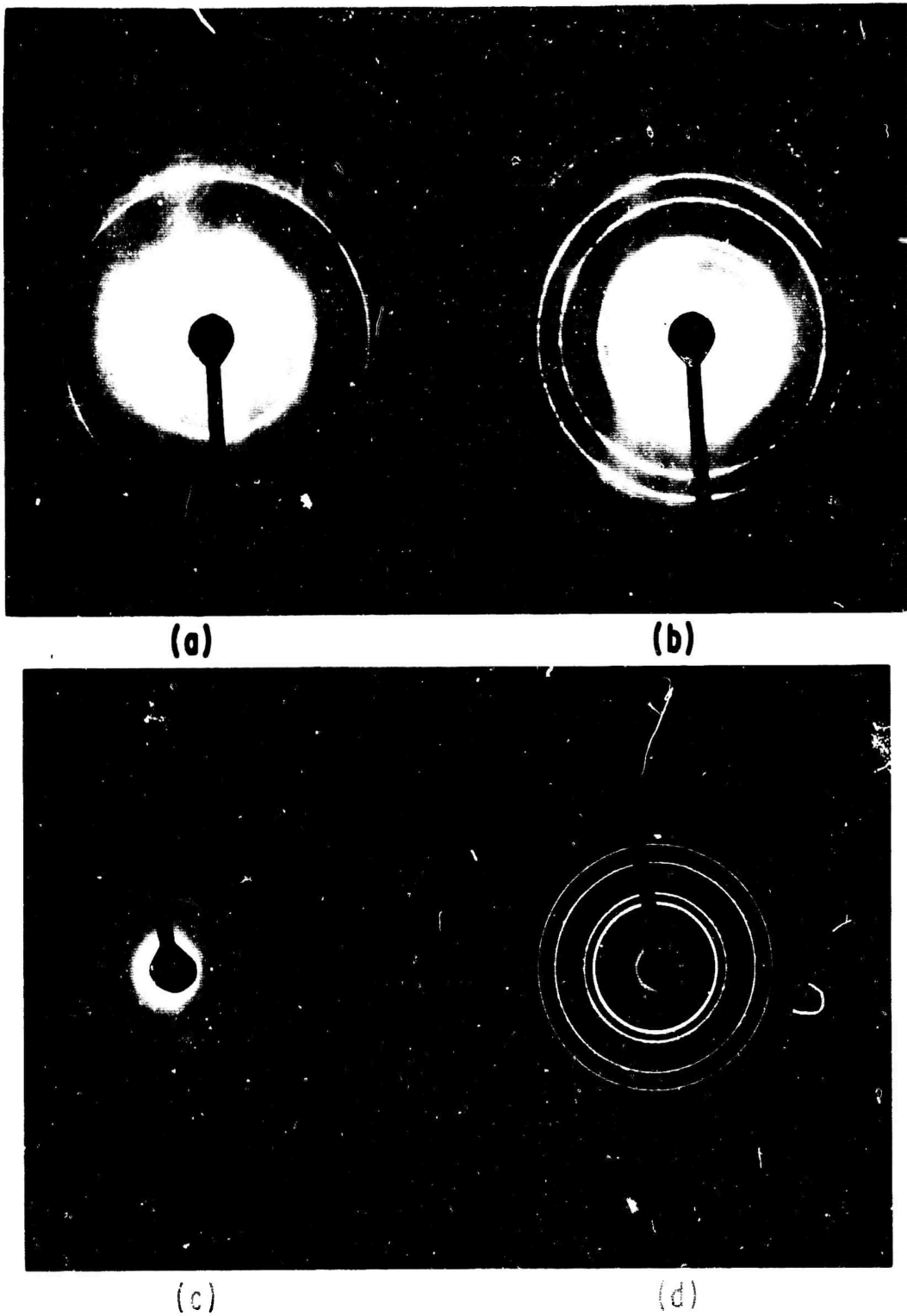


Fig. 10. Electron Diffraction Patterns of: (a) Post-Exposure Surface Material, (c) Highly Oriented Graphite, and (b) and (d) Gold Standards.

according to the crystalline ordering near the surface, resulting in the observed etch. This effect is likely to take place only where large temperature gradients are present. During oxidation the opposite effect is expected. The gradients have no significant effect, and any protuberance would recede faster than the base surface because of their increased area-to-volume ratio.

B. NORMAL SPECTRAL REFLECTANCE AT ROOM TEMPERATURE

A standard Gier Dunkle integrating sphere reflectometer* was used to check the near-normal reflectance as a function of wavelength $R_N(\lambda)$ through the range from visible wavelengths to 2.2μ . $R_N(\lambda)$ was measured for four PG surfaces (Fig. 11): (1) as received from the manufacturer, (2) after heating in argon, (3) after heating to $\sim 2000^\circ\text{C}$ in stagnant air, and (4) after reaching a temperature of $\sim 2900^\circ\text{C}$ when exposed to a subsonic air plasma jet.

The sample surfaces for (1) and (2) were those of the emittance samples and, therefore, cylindrical. Small chips from these samples were placed in the reflectometer. The optics were masked to conform to the sample sizes. The angle of incidence was varied in the range from 0 to 30 deg and set near 20 deg to avoid any serious specular reflection back out of the sphere. The samples used for steps (3) and (4) came from the thick PG plates. Three of the surfaces gave fairly similar $R_N(\lambda)$ results; the fourth, etched in argon, exhibited a markedly lower $R_N(\lambda)$.

From these measurements and since at 2800°C nearly 80% of the energy of a blackbody is radiated at wavelengths shorter than 2.2μ , one can predict a large increase in ϵ_H as a result of the etching.

*

Gier Dunkle Instruments, Inc., Santa Monica, California.

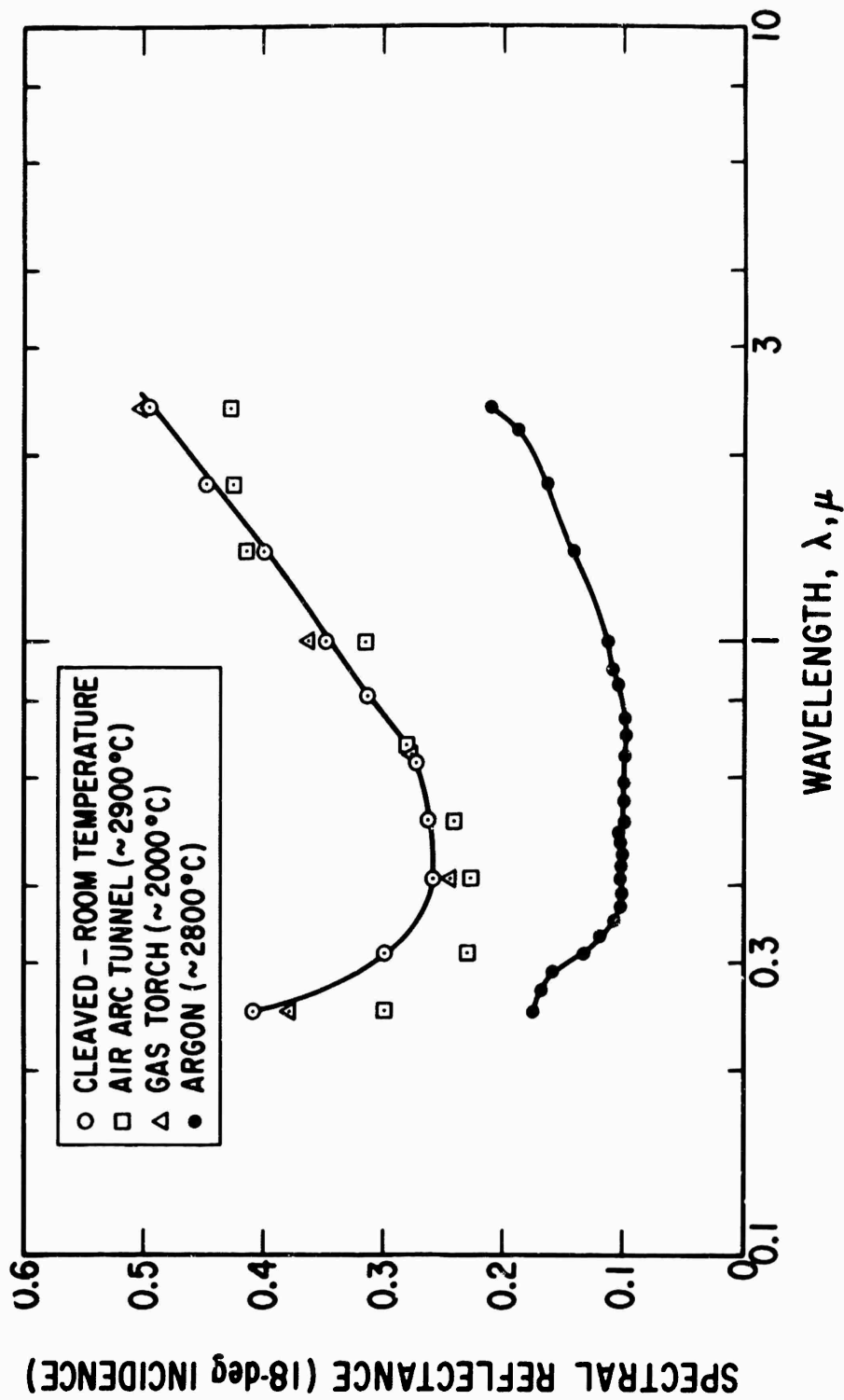


Fig. 11. Spectral Reflectance at 18-deg Incidence of PG Surfaces After Various Exposures

C. NORMAL EMITTANCE AT 0.65 μ

The $\log(\Delta T_{\text{obs}})$ vs T_i is shown in Fig. 12 for one sample; for the same sample, $\log W$ vs T_i is shown in Fig. 13. After etching the surface to various degrees, arbitrarily labeled I to V, low-temperature data were taken. In general, little effect on ΔT_{obs} was seen but the effect of the surface condition is clearly visible in the W plot. The change from I to II took place typically near a 2540°C surface temperature in about 1 min, thereafter settling to some degree. The changes from II to V took place at increasingly higher threshold temperatures to 2790°C , with the times decreasing to 10 or 20 sec. Investigations above 2800°C were prevented by sample failure. The possibility that changes in k_c are responsible is ruled out with confidence from a comparison of the data for the largest and the smallest t for similar outside temperature histories. For instance, the steps described consistently took place at the same brightness temperatures, despite the fact that the inner layers of PG for the thick PG samples were hundreds of degrees higher than those in the thin PG samples.

An explanation based on the possible formation of cracks was discarded upon microscopic examination of sample cross sections after the high-temperature runs. Some of the thinnest samples, with thickness-to-diameter ratios near 370:1, exhibited no cracks and, yet, were consistent in the ΔT_{obs} changes.

It should be pointed out that the mere reproducibility of ΔT_{obs} in no way implies that ϵ_N (0.65μ) is constant while ϵ_H changes. In fact, the emittances change simultaneously. The resistivity of the samples was found to be quite reproducible within the time-temperature exposures and was used as a double check.

The $(\Delta T_{\text{obs}} - \Delta T_{\text{ATJ}})$ values for the various samples were graphed vs $f(t)$ for equal W levels and similar surface finishes. Typical graphs are shown in Fig. 14. Similar plots were done for each surface condition (i. e., I to V), although the degree of etching was not identical

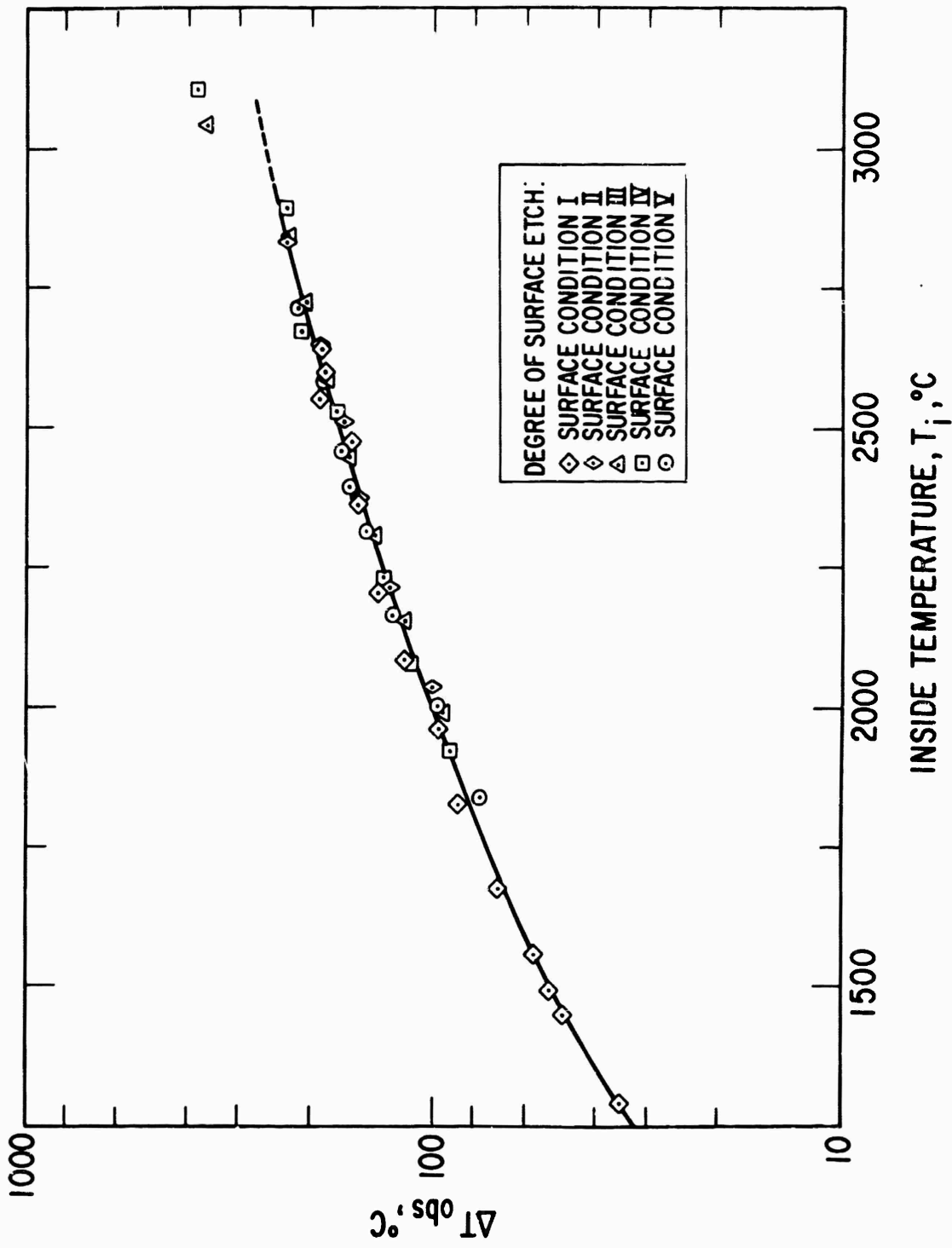


Fig. 12. Typical Plot of ΔT_{obs} vs T_i .

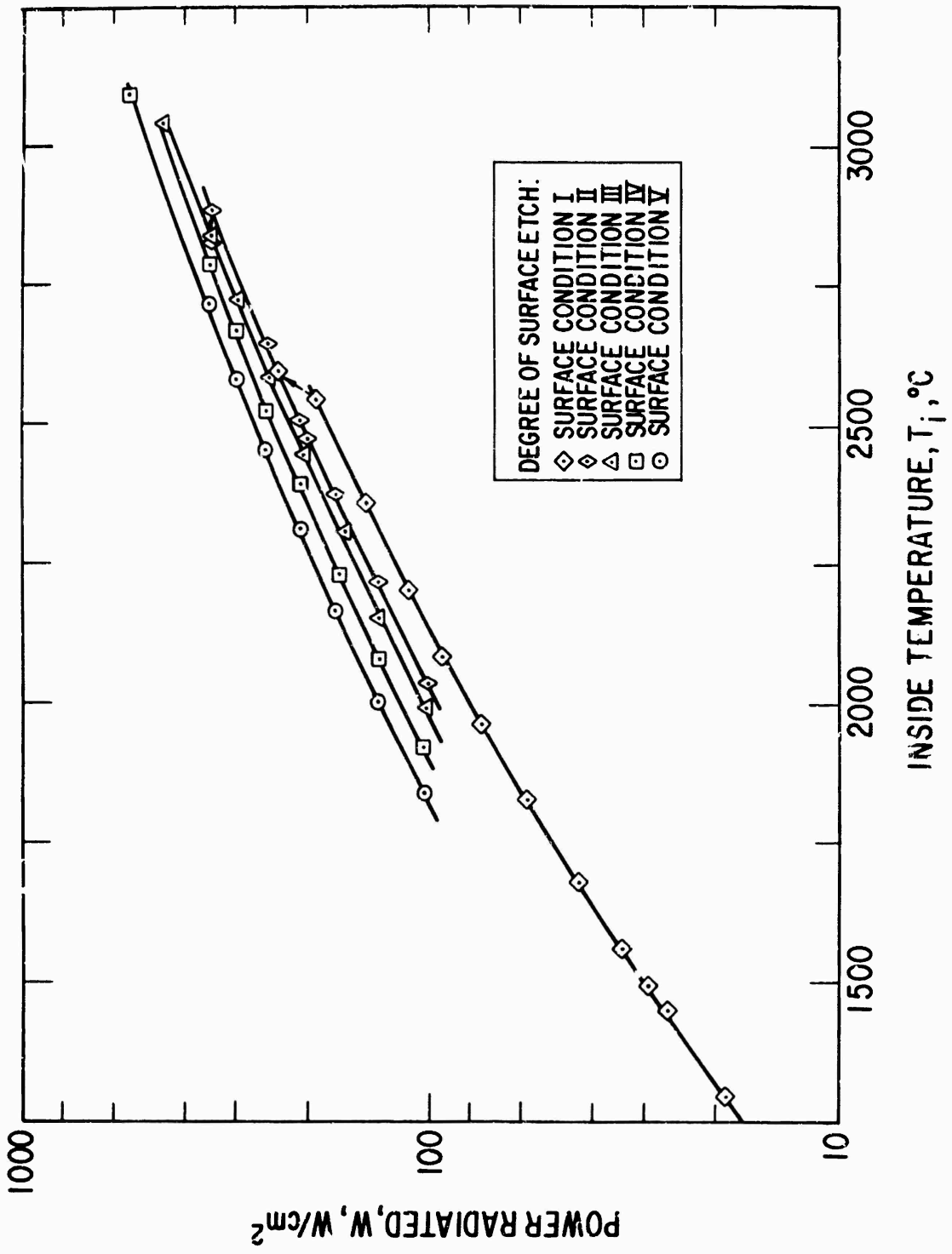


Fig. 13. Typical Plot of Measured W vs T_i .

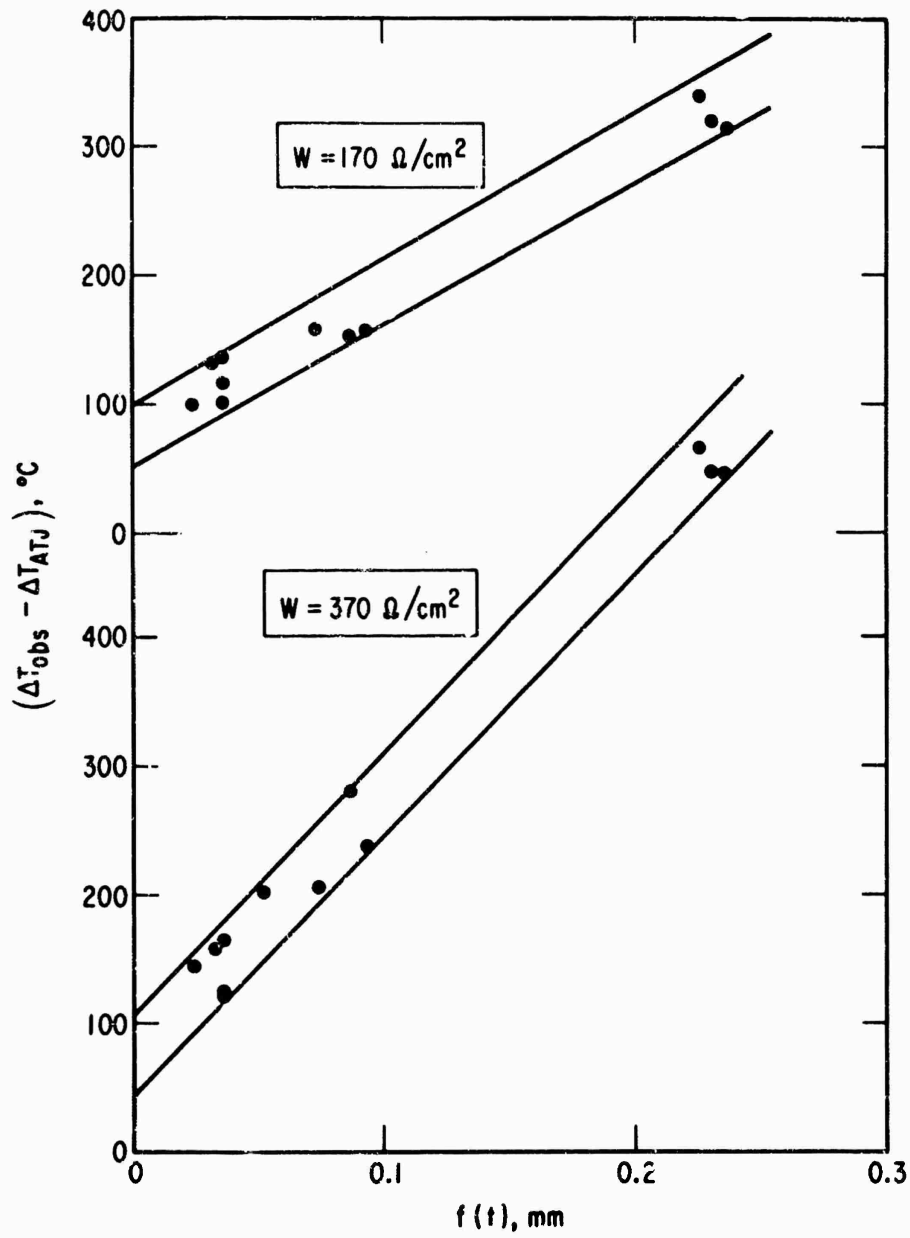


Fig. 14. Examples of $(\Delta T_{\text{obs}} - \Delta T_{\text{ATJ}})$ vs $f(t)$ Plots.

in all cases. The values of $\epsilon_N(0.65 \mu)$ from the zero intercepts are shown in Fig 15; the effect of etching is clearly seen.

D. TOTAL HEMISPHERICAL EMITTANCE

The ϵ_H was calculated from $\epsilon_N(0.65 \mu)$ with Eqs. (1), (2), and (3). The results (Fig. 15) show a more pronounced increase in ϵ_H than in $\epsilon_N(0.65 \mu)$. The apparent ϵ_H departure from approximate linearity at low temperatures is due to the increasing contribution of the undesired axial conduction to the cool electrodes (Fig. 16). A similar increase at the very high temperatures, particularly where the ϵ_H for the Condition V surface appears to exceed 1, is due to the power consumed in subliming the material. Calculations of this power were made based on vapor pressure measurements extrapolated from low temperature data such as those described in Ref. 4. The results, while unreliable due to the extrapolation, do predict the apparent increase observed in ϵ_H .

E. THERMAL CONDUCTIVITY IN THE c-DIRECTION

Partial separation of the PG from the ATJ was suspected, particularly for thick PG layers, because of the difference in the thermal expansion coefficients of the two graphites. A few of the thick samples were tapped with a hammer to loosen the contact at the interface and to crack the ATJ inside. Thus, PG shells were obtained that had been deposited at the same time as the PG/ATJ samples with equivalent thicknesses and were identical to them in every way except for the substrate absence.

If the ΔT_{obs} and W are known for two samples, one with and one without substrate, an expression can be written and solved for k_c explicitly. Experimental data gave no solution. This discrepancy is ascribed to a partial separation at the interface. The conductivity of the assumed gap was evaluated from the data and followed approximately the T^3 dependence that the equivalent conductivity of a gap would follow in a gray body where thermal radiation is the predominant mode of heat transfer.

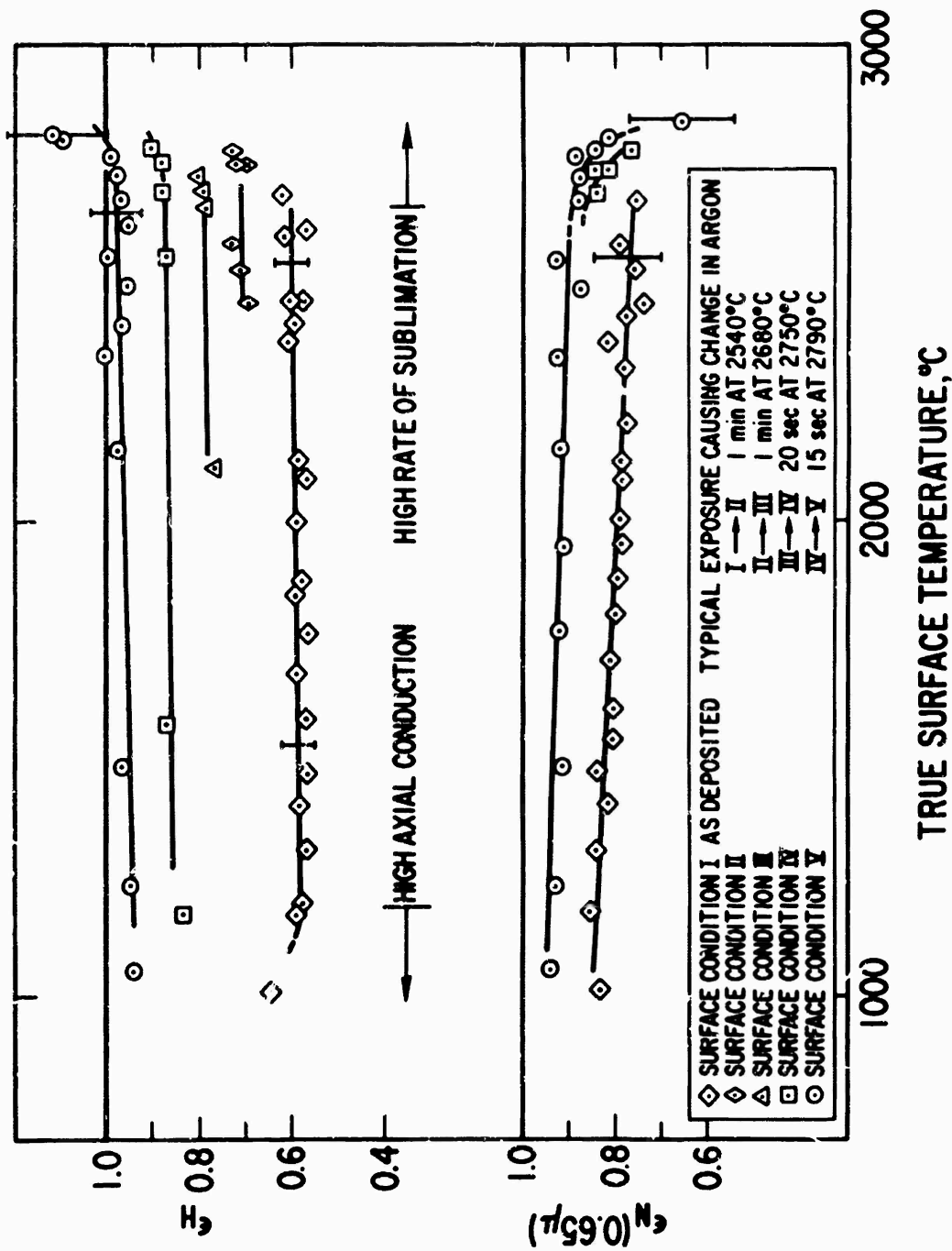


Fig. 15. Total Hemispherical Emittance and Normal Emittance of PG Samples at 0.65 μ .

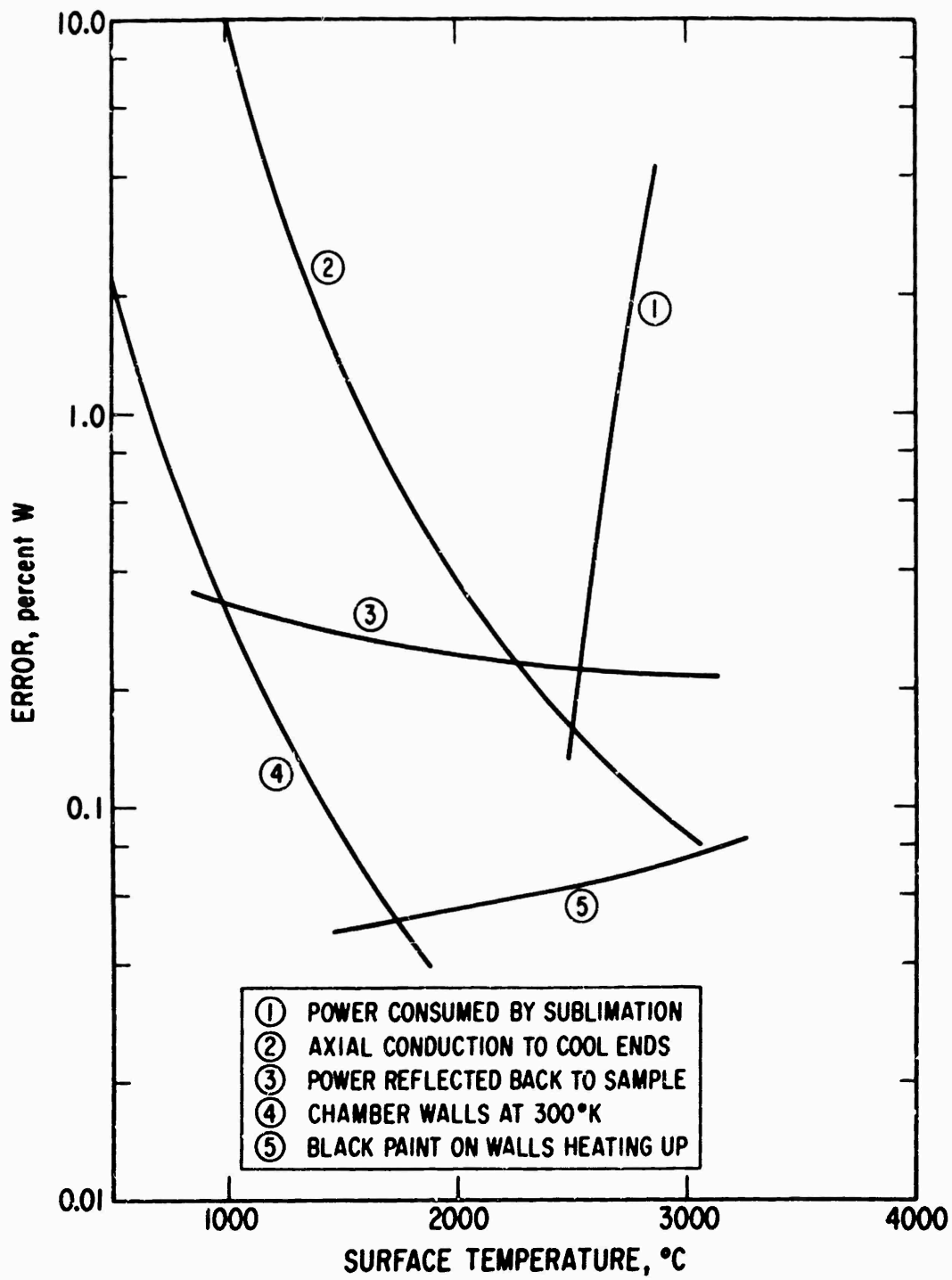


Fig. 16. Systematic Errors in ϵ_H for a Typical Sample.

The ΔT_{obs} for the thick PG samples were therefore corrected empirically so as to eliminate the effect of the crack before inclusion in the plots of $(\Delta T_{\text{obs}} - \Delta T_{\text{ATJ}})$ vs $f(t)$. This correction decreased with increasing temperature to a nearly negligible amount at highest temperatures, in keeping with the gap postulate.

The ϵ_N (0.65 μ) data were used to calculate k_c for the PG shells without substrate by applying Eq. (5). The resulting k_c (Fig. 17) for the shells increases with temperature above 1600°C. An increase has been observed by other experimenters for cylindrical samples rather than flat plates.*

The ΔT_{obs} data have too much scatter to deduce the k_c of the thin PG samples with sufficient precision to investigate the behavior of k_c with t .

It is felt that the validity of these conductivity data is restricted to the samples tested and not representative of any other material. The large anisotropy of PG in expansion coefficient coupled with the enormous thermal gradients in the PG layer would give rise to significant strains and the production of defects in the crystalline structure, which are inherent in nonflat samples.

F. ELECTRICAL RESISTIVITY IN THE ab -PLANE

This property as determined for the samples used here is subject to large uncertainties. The thickness t and the geometry of the ATJ substrate can be measured within a few percent. However, a given error in the measurement of the ATJ outside diameter can result in a proportional error in ρ_{ab} one order of magnitude higher. Consequently, the ρ_{ab} values obtained for the thick PG samples (Figs. 18 and 19) show considerable scatter and variation in slope.

* Private communication, C. D. Pears, Southern Research Institute, Birmingham, Alabama.

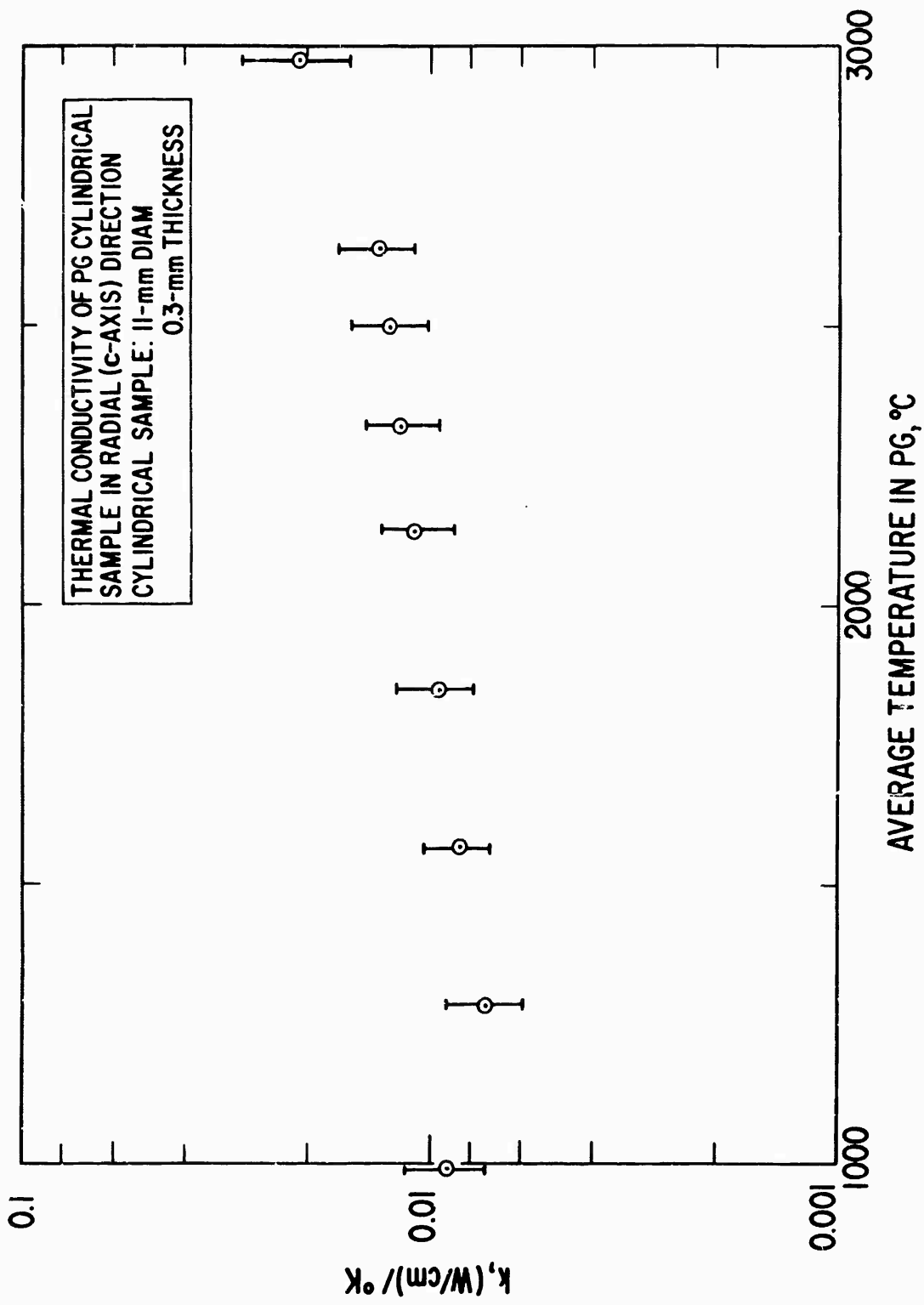


Fig. 17. Thermal Conductivity of PG Cylindrical Sample in Radial (c-Axis) Direction.

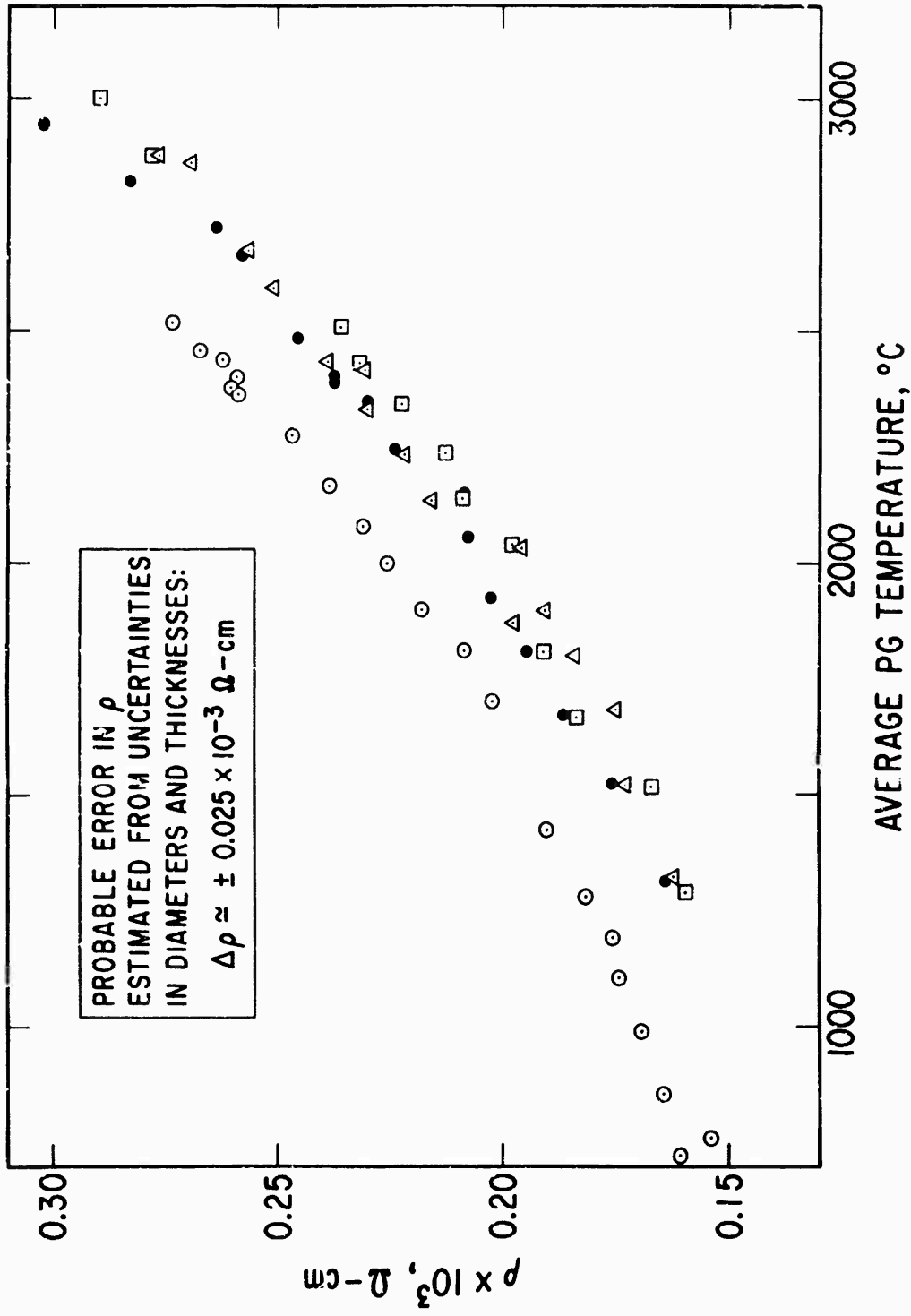


Fig. 18. Electrical Resistivity in *ab*-Direction Calculated from Four PG Shell and PG-AIJ Samples with $t \approx 0.3$ mm.

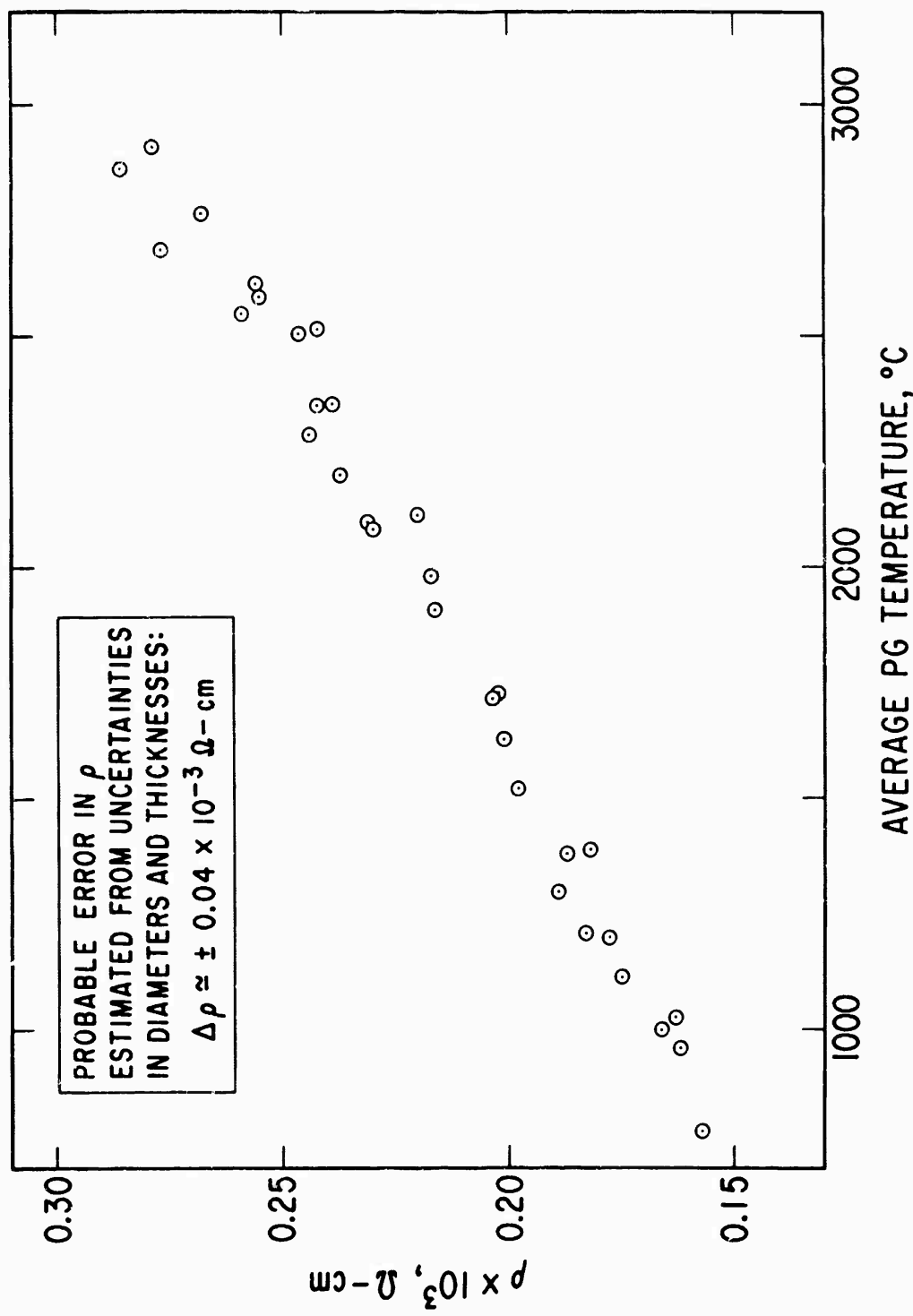


Fig. 19. Electrical Resistivity in the ab-Direction Calculated for a PG-ATJ Sample with Medium Thickness ($t \approx 0.081$ mm).

V. CONCLUDING REMARKS

This discussion is limited to the interpretation of results for ϵ_H and ϵ_N (0.65μ). The theoretical validity of the emittances measured is open to question due to the inevitable presence of thermal gradients at the surfaces and moreover to the fact that the electrical heating current flowed along the ab-plane (i. e., orthogonal to the direction of the measured radiation). The very low thermal conductivity of PG in the c-direction, which makes it an attractive insulator, also inhibits study of some of its thermal radiation properties. The emittances require theoretically isothermal conditions and, at least for practical measurements, nearly isothermal regions. In contrast, the temperature gradients observed in some of the samples exceeded $1000^\circ\text{C mm}^{-1}$ along the c-direction. All of the visible emission, however, originated within depths of the order of 10^{-4} mm (calculated from published optical constants).

The engineering applicability of the present data on ϵ_H and ϵ_N (0.65μ) depends to a great extent on the reproducibility of surface finishes. A useful criterion for evaluating surface differences is the normal spectral reflectance, which is measured with relative ease at room temperature. Accordingly, in the presence of an oxidizing atmosphere, the data measured on the test sample surfaces with "as deposited" finish should apply. In other environments, such as space, a decrease in the specularity when the surface is heated may cause results that are comparable to those observed in these tests.

REFERENCES

1. C. D. Pears, Summary Report to Lockheed Missiles and Space Company, Rpt. No. 6216-1209-XVII, Southern Research Institute, Birmingham, Alabama (November 1961).
2. Marple, Pyrolytic Graphite Engineering Handbook, Specialty Alloys Section, Metallurgical Products Department, General Electric Company, Detroit, Michigan (May 1964).
3. J. H. Richardson and E. H. Zehms, Structural Changes in Pyrolytic Graphite at Elevated Temperatures, TDR-269(4240-10)-3, Aerospace Corp., El Segundo, California (December 1963).
4. R. J. Thorn and G. H. Winslow, Vaporization Coefficient of Graphite and Composition of the Equilibrium Vapor, J. Chem. Phys. 26, (1) 186 (1957).

UNCLASSIFIED
Security Classification

DOCUMENT CONTROL DATA - R&D		
<i>(Security classification of title, body of abstract and indexing annotation must be entered when the overall report is classified)</i>		
1 ORIGINATING ACTIVITY (Corporate author) Aerospace Corporation El Segundo, California	2a REPORT SECURITY CLASSIFICATION Unclassified	2b GROUP
3 REPORT TITLE BASAL PLANE EMITTANCE OF PYROLYTIC GRAPHITE AT ELEVATED TEMPERATURES		
4 DESCRIPTIVE NOTES (Type of report and inclusive dates)		
5 AUTHOR(S) (Last name, first name, initial) Champetier, Robert J.		
6. REPORT DATE July 1967	7a TOTAL NO. OF PAGES 44	7b. NO. OF REFS 3
8a. CONTRACT OR GRANT NO. F04695-67-C-0158	9a. ORIGINATOR'S REPORT NUMBER(S) TR-0158(3250-20)-10	
b. PROJECT NO.	9b. OTHER REPORT NO(S) (Any other numbers that may be assigned this report) SAMSO-TR-67-5	
c.		
d.		
10. AVAILABILITY/LIMITATION NOTICES This document has been approved for public release and sale; its distribution is unlimited.		
11. SUPPLEMENTARY NOTES	12. SPONSORING MILITARY ACTIVITY Space and Missile Systems Organization Air Force Systems Command Los Angeles, California	
13. ABSTRACT A direct measurement of the total hemispherical emittance of "as deposited" PG layers on ATJ graphite cylinders in the range from 1200 to 2840°C is described. The method consisted of resistively heating these long, thin cylinders inside a cooled, blackened enclosure until the power generated was all radiated and temperature equilibrium ensued. By sighting an optical pyrometer through a window in the enclosure, the apparent temperature of the surface and the true temperature of a cavity inside the samples could be measured. These temperatures, as well as the electrical power supplied to the sample, were recorded for each equilibrium temperature. These data for various sample thicknesses were used to determine the true temperature of the surface, the total hemispherical emittance ϵ_H , and the normal emittance at 0.65 μ . The electrical resistivity in the ab-plane and the thermal conductivity in the c-direction were also determined. The ϵ_H for PG was approximately 0.6 μ from 1300 to 2600°C. Exposure for a few seconds in an inert atmosphere or in a vacuum to temperatures above 2600°C, irreversibly altered the surface finish and increased ϵ_H to progressively higher values depending on the time and temperature. The normal emittance values at 0.65 μ also were significantly affected.		

DD FORM 1473
(IF ACSIMILE)

UNCLASSIFIED
Security Classification

14.

KEY WORDS

Emittance, Thermal
Pyrolytic Graphite, Reflectance
Pyrolytic Graphite, Emittance
Pyrolytic Graphite, Resistivity
Pyrolytic Graphite, Thermal Conductivity
Pyrolytic Graphite, High-Temperature Behavior
Temperature Measurement

Abstract (Continued)